Award Number: W81XWH-13-1-0295

TITLE: Therapeutic and Imaging Applications of Dopamine Receptor Agonists in Breast Cancer

PRINCIPAL INVESTIGATOR: Nira Ben-Jonathan

CONTRACTING ORGANIZATION: University of Cincinnati
Cincinnati, OH 45267

REPORT DATE: September 2015

TYPE OF REPORT: Annual

PREPARED FOR: U.S. Army Medical Research and Materiel Command
Fort Detrick, Maryland 21702-5012

REPORT DOCUMENTATION PAGE

Form Approved
OMB No. 0704-0188

1. REPORT DATE
September 2015

2. REPORT TYPE
Annual

3. DATES COVERED
1Sep2014 - 31Aug2015

4. TITLE AND SUBTITLE
Therapeutic and Imaging Applications of Dopamine Receptors in Breast Cancer

5a. CONTRACT NUMBER
W81XWH-13-1-0295

5b. GRANT NUMBER
BC122992

5c. PROGRAM ELEMENT NUMBER

6. AUTHOR(S)
Nira Ben-Jonathan

E-Mail: Nira.Ben-Jonathan@uc.edu

5d. PROJECT NUMBER

5e. TASK NUMBER

5f. WORK UNIT NUMBER

7. PERFORMING ORGANIZATION NAME(S) AND ADDRESS(ES)
University of Cincinnati
3125 Eden Ave
Cincinnati, OH 45267

8. PERFORMING ORGANIZATION REPORT

9. SPONSORING / MONITORING AGENCY NAME(S) AND ADDRESS(ES)

U.S. Army Medical Research and Materiel Command
Fort Detrick, Maryland 21702-5012

10. SPONSOR/MONITOR'S ACRONYM(S)

11. SPONSOR/MONITOR'S REPORT NUMBER(S)

12. DISTRIBUTION / AVAILABILITY STATEMENT

Approved for Public Release; Distribution Unlimited

13. SUPPLEMENTARY NOTES

14. ABSTRACT

Patients with advanced breast cancer either do not respond to anti-hormonal therapy or develop resistance to chemotherapy, providing major incentives to seek novel therapies that circumvent these drawbacks. Dopamine (DA) is a catecholamine which acts as a neurotransmitter in the brain and as a hormone in the periphery. DA binds to five receptors, D2-like (D2, D3 and D4) and D1-like (D1 and D5). Our data show that D1R is overexpressed in breast carcinomas while adjacent normal breast tissue is D1R-negative. Fenoldopam, a potent D1R agonist, was highly effective in suppressing xenograft growth in mice, by increasing both apoptosis and necrosis. An imaging system for detecting D1R-expressing breast tumors has been developed, albeit it requires additional improvements. These data suggest that D1R analysis in tumor biopsies could serve as a prognostic biomarker for advanced breast cancer. Moreover, Fenoldopam, an FDA approved, selective D1R agonist which does not penetrate the brain, should be exploited as a novel therapeutic agent in patients who do not respond to standard of care therapy.

15. SUBJECT TERMS
Dopamine receptors, primary tumors, apoptosis, fenoldopam

16. SECURITY CLASSIFICATION OF:			17. LIMITATION OF ABSTRACT	18. NUMBER OF PAGES	19a. NAME OF RESPONSIBLE PERSON USAMRMC
a. REPORT	b. ABSTRACT	c. THIS PAGE			19b. TELEPHONE NUMBER *(include area code)*
Unclassified	Unclassified	Unclassified	Unclassified	18	

Standard Form 298 (Rev. 8-98)
Prescribed by ANSI Std. Z39.18

Table of Contents

Introduction

Background

Many patients with advanced breast cancer either do not respond to anti-hormonal therapy or develop resistance to chemotherapy, providing major incentives to seek novel therapies that circumvent these drawbacks (1). Dopamine (DA) is a catecholamine which acts as a neurotransmitter in the brain (2), and as a hormone in the periphery (3). DA binds to five receptors, D2-like (D2, D3 and D4), classified by the inhibition of cAMP, and D1-like (D1 and D5), classified by the stimulation of cAMP (4). We discovered a robust expression of D1R in breast cancer cell lines (BCC) and in primary breast carcinomas. Our data demonstrated that treatment of D1R-expressing BCC with low nanomolar doses of D1R selective agonists, caused apoptosis and sensitized the cells to cytotoxicity by doxorubicin, a potent chemotherapeutic agent (5). Moreover, preliminary data showed that Fenoldopam (Fen), an FDA-approved, selective D1R agonist which does penetrate the brain (6), suppressed the growth of D1R-expressing breast cancer xenografts in nude mice.

Hypothesis

D1R overexpression in breast cancer serves as a molecular biomarker which can be leveraged, through the use of D1R agonists, as a novel therapy for suppressing tumor growth and reducing resistance to chemotherapy.

Objectives for year 02

Aim 1: To compare D1R expression in primary breast carcinomas and adjacent normal breast tissue and examine the consequences of D1R knockdown.

Aim 2: To characterize the effects of fenoldopam on growth of xenografts derived from MDA-MB-231 cells.

Aim 3: To establish imaging methods for detecting D1R-expressing tumors.

Body

Expression of D1R in primary breast carcinomas and normal breast tissue

The *DRD1* transcript was cloned from MDA-MB-231 breast cancer cells (BCC) and was found identical to the published sequence. Next, 14 primary breast carcinomas and matched normal breast tissue from the same individuals were analyzed for *DRD1* gene expression by RT-PCR (**Fig 1a**), and D1R proteins by Western blotting

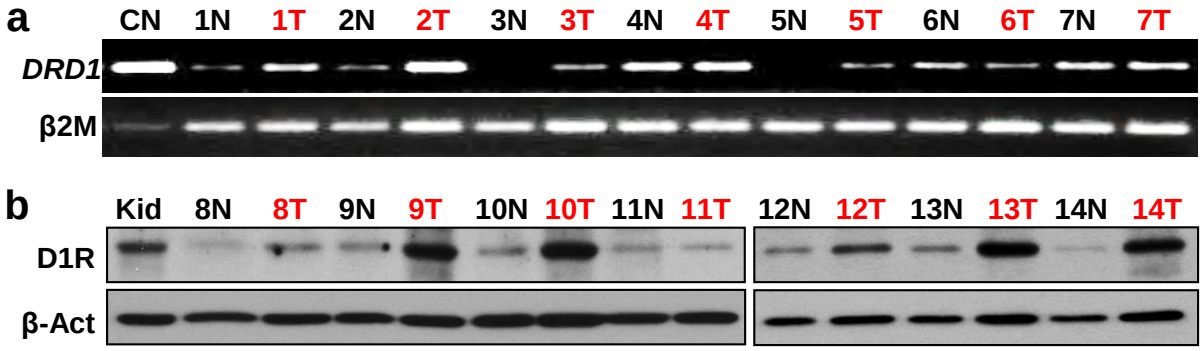

Fig 1. D1R expression in primary breast carcinomas. *DRD1* gene (a) and protein (b) expression in tumors (T) and matching normal breast tissue (N), as determined by qPCR and Western blotting respectively. CN: caudate nucleus, β2M: β2-microglobulin, Kid: kidney, β-Act: β-Actin.

(**Fig 1b**). As evident in **Fig 1**, *DRD1* expression was higher in tumors than in normal breast in 4/7 samples, while tumor D1R proteins were higher in 6/7 samples. These data confirm overexpression of D1R in a large number of carcinomas as compared to adjacent normal breast tissue.

Effects of *DRD1 knockdown and validation of the rabbit monoclonal antibodies against D1R*

Given the reports on lack of specificity of many commercially available antibodies against dopamine receptors (7), it was found necessary to validate the rabbit anti-D1R monoclonal antibodies (mAb) used here. First, antibody pre-absorption with the immunizing peptide abolished the D1R bands in BCC lysates (data not shown). Next, we conducted knockdown of the receptor using shRNA. *DRD1* knockdown by shRNA in MDA-MB-231 cells (**Fig 2a**) and HEK293T cells (**Fig 2b**), markedly decreased the D1R protein band (**Figs 2c** and **2d** respectively); D1R knockdown did not affect D2R protein levels in MDA-MB-231 cells (data not shown). To

determine the functional consequence of D1R knockdown, MDA-MB-231 cells with downregulated D1R were incubated with Fenoldopam (Fen) and cell viability was analyzed 4 days later. As evidence in **Fig 2e**, Fen was

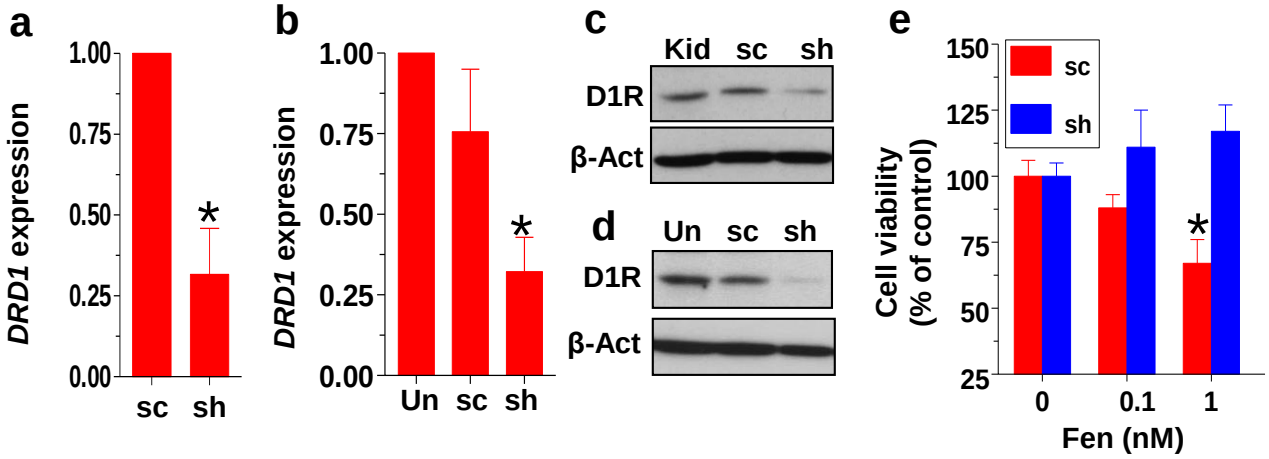

Fig 2. (a) *DRD1* gene knockdown in MDA-MB-231 cells transfected with scrambled (sc) or *DRD1* shRNA (sh). Data are presented as relative changes vs. sc cells (means±SEM, n=5. *P<0.01). (b) *DRD1* gene expression in untransfected (Un), or transiently transfected HEK293T cells with sc or sh sequences. Data are presented as relative changes vs. Un cells (means±SEM. n=3. *P<0.01). Reduced D1R proteins in MDA-MB-231 (c), and HEK293T (d) cells, transfected with *DRD1* shRNA. (e) *DRD1* knockdown in MDA-MB-231 cells abrogated the suppression of cell viability by Fenoldopam (Fen). Cells transfected with scrambled or *DRD1* shRNA were incubated with Fen for 4 days and cell viability was analyzed by resazurin (means±SEM, n=6. *P<0.05).

ineffective as a suppressor of cell viability in cells that do not express D1R, lending further supports to its specificity as a D1R agonist.

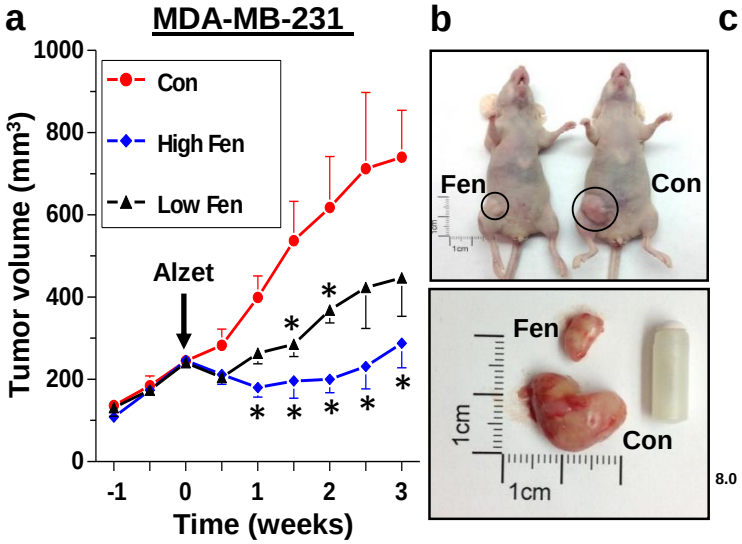

Fig 3. Fenoldopam Inhibits tumor growth in a mouse xenograft model. (a) Fen suppresses the growth of orthotopic MDA-MB-231 xenografts. Mice were implanted with Alzet pumps delivering vehicle (Con), high Fen (400 ng/kg/min) or low Fen (133 ng/kg/min) for 3 weeks (means±SEM, n=7-8 mice. *P<0.05). (b) Mice with control- and high Fen-treated tumors, and the same tumors, pictured with an Alzet pump, removed after 3 weeks.

Suppression of xenograft growth by Fenoldopam

The next objective was to determine the *in vivo* effects of Fen on tumor growth. Because of the short half life of Fen in the circulation (8), it was decided that the optimal delivery of Fen should be via implantable Alzet osmotic mini-pumps. Eight-week old female athymic *nu/nu* mice were housed 4/cage in sterile cages, and were acclimated for 7-10 days before experiments. MDA-MB-231 cells (1.5 x 10^6 cells/60µl) were suspended 1:1 in PBS/Matrigel and inoculated into the inguinal mammary fatpad. Tumor dimensions were measured twice/week and tumor volume were calculated as length x $width^2$ x 0.52.

Power calculation, based on previous studies in our lab, predicted a 80% chance of finding significant differences (α= 0.05, power of 0.8) when using 8 mice/treatment. Mice were randomized among treatments. When tumors were 200-250 mm^3 in volume, Alzet mini-pumps with a 100 µl reservoir, rated for a continuous delivery at 0.11 µl/hr for 4 weeks, were implanted sc in the dorsal neck. The pumps delivered PBS (control), high Fen (400 ng/kg/min), calculated to generate serum levels of ~30 nM or low Fen (133 ng/kg/min; 10 nM). As shown in **Fig 3a**, within one week, Fen at high-dose significantly reduced tumor volume, while the low dose had an intermediate effect. **Fig 3b** shows photographs of fen-treated and control mice treated for 3 weeks, treated tumors and a photograph of an Alzet pump.

Induction of both apoptosis and necrosis by Fenoldopam

Three weeks after initiation of treatment with Fenoldopam, mice were sacrificed and tumors were removed and

weighed. Tumors were fixed in paraformaldehyde, embedded in paraffin, sectioned and mounted on slides. The percent of apoptotic cells was then determined by a TUNEL assay, while the necrotic areas were quantified by histopathology. As demonstrated in **Fig 4**, Fen at high dose significantly reduced tumor weight, and this occurred by increasing both apoptosis and necrosis. A combination of apoptosis and necrosis is likely responsible for the more robust effects of Fen *in vivo* than *in vitro*. Tumor necrosis could be due to activation of multiple pathways within tumor cells, some of which can suppress angiogenesis. Notably, both doses of Fen are within the range of its serum levels in hypertensive patients treated with Fenoldopam.

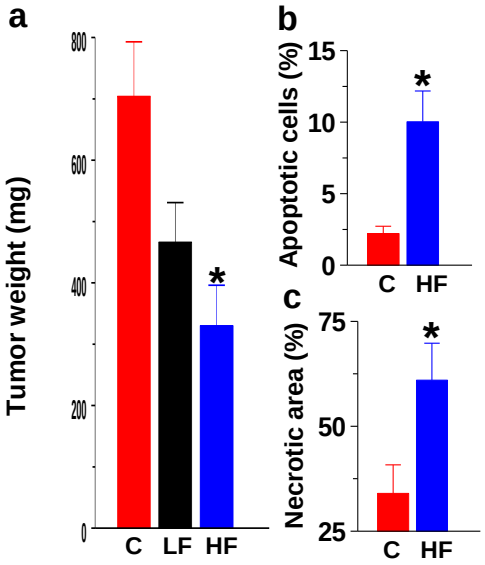

Fig 4. Fenoldopam suppresses tumor growth by increasing both apoptosis and necrosis. After 3 weeks, tumors were removed and weighed (a), and analyzed by TUNEL for apoptosis (b) and by histopathology for necrosis (c). C: control; LF; low dose Fen; HF: high dose Fen. See **Fig 3** for other details.

In vivo imaging of D1R-expressing tumors

One of our major objectives was to develop a method for *in vivo* imaging for the detection of D1R-expressing tumors, which could eventually be used for tumor diagnosis and prognosis in breast cancer patients. As proof of principle, we took advantage of the highly specific Rabbit anti-D1R mAb. The mAb were conjugated to Alexa Fluor 647, using an antibody Labeling Kit. The fluorescent mAb (100 µg proteins) were then injected via tail vein into mice with MDA-MB-231-derived inguinal tumors of moderate size. Mice were imaged 24 hrs after the injection, using Kodak Multispectral Imaging instrument. As shown in **Fig 5**, one mouse had intense fluorescence at the tumor site, while another also has fluorescence in distal metastases, as confirmed histologically. Rabbit IgGs labeled with Alexa Fluor 647 and injected into mice showed no specific fluorescence in the tumors (not shown). Since these antibodies do not recognize mouse D1R, no D1R-expressing mouse tissue are seen.

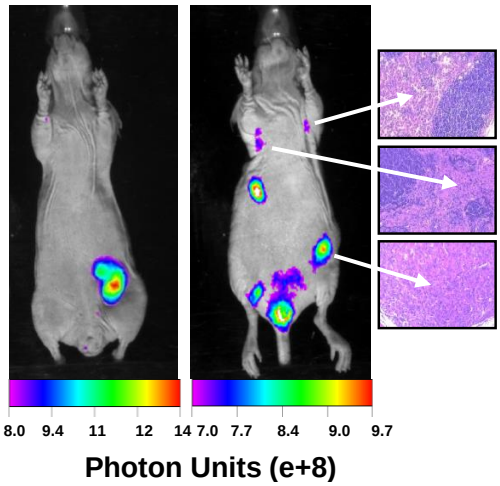

Fig 5. Fluorescence imaging of D1R-expressing tumors and metastases. Mice with MDA-MB-231 xenografts were *iv* injected with human anti-D1R antibody conjugated to Alexa-Fluor 647. *In vivo* imaging after 24 hrs shows intense fluorescence of the primary tumors and metastases. Arrows indicate insets of H&E staining of primary tumor and metastases in the axillary lymph nodes.

Development of PET imaging

Due to the poor penetration of fluorescence signals, this method is not adequate for imaging deep-seated breast tumors. Instead, we wished to develop positron-emission tomography (PET), which is commonly used to diagnose disturbances in dopamine receptors in the brain, and is also showing increasing relevance to the detection and treatment of breast cancer (9). The only ligand with high selectivity for D1R that is suitable for PET is TISCH [(+-)-7-chloro-8-hydroxy-1-(3'-iodophenyl)-3-methyl- 2, 3, 4, 5-tetrahydro-1H-3-benzazepine]; (10)). Since TISCH is not commercially available, we have contacted many chemical companies, and finally identified one company (Science Exchange in Palo Alto CA) which has agreed to custom-synthesize a TISCH precursor (costing us $10,000), which can be radiolabeled with ^{124}I for PET imaging, as illustrated in **Fig 6**. Radiolabeling, purification, verification of binding of the labeled ligand to D1R and the subsequent use of this compound in xenograft-bearing mice will be undertaken next year.

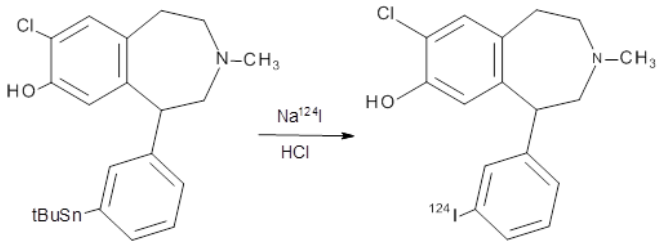

Fig 6. Chemical reaction for TISCH labeling of with ^{124}I.

Key Research Accomplishments

- Demonstrated overexpression of D1R in the majority of breast carcinomas examined, while adjacent normal breast tissue was D1R-negative.
- Knockdown of D1R in two cell lines assisted in the validation of the specificity of the monoclonal antibodies

used to detect D1R, and demonstrated their inability to respond to the suppressive effects of Fenoldopam.

- A continuous infusion of Fenoldopam into mice with MDA-MB-231 xenografts effectively suppressed tumor growth, by inducing both apoptosis and necrosis.
- Developed a proof of concept fluorescence imaging method for detecting D1R-expressing breast tumors.
- Ongoing studies are developing a PET imaging system which is more suitable than fluorescence imaging for diagnosis and prognosis in breast cancer patients.

Reportable outcome

A manuscript entitled: Expression and Therapeutic Targeting of Dopamine Receptor-1 (D1R) in Breast Cancer" by Dana C. Borcherding, Wilson Tong, Eric R. Hugo, David F. Barnard, Sejal Fox, Kathleen LaSance, Elizabeth Shaughnessy, and Nira Ben-Jonathan, was accepted for publication in Oncogene (Appendix 1).

Conclusion

D1R is overexpressed in breast carcinomas but not in normal breast tissue. Fenoldopam a potent D1R agonist, was highly effective in suppressing tumor growth in mice by increasing both apoptosis and necrosis. An imaging system for detecting D1R-expressing breast tumors is feasible, albeit it requires additional improvements. These data suggest that D1R analysis in tumor biopsies could serve as a prognostic biomarker for advanced breast cancer. Moreover, Fenoldopam, an FDA approved, potent D1R agonist which does not penetrate the brain, should be exploited as a novel therapeutic agent in patients who do not respond to standard of care therapy.

Appendix 1

Accepted manuscript on line (Oncogene)

References

1. Coley HM 2008 Mechanisms and strategies to overcome chemotherapy resistance in metastatic breast cancer. Cancer Treat Rev 34:378-390
2. Kienast T, Heinz A 2006 Dopamine and the diseased brain. CNS Neurol Disord Drug Targets 5:109-131
3. Amenta F, Ricci A, Tayebati SK, Zaccheo D 2002 The peripheral dopaminergic system: morphological analysis, functional and clinical applications. Ital J Anat Embryol 107:145-167
4. Beaulieu JM, Gainetdinov RR 2011 The physiology, signaling, and pharmacology of dopamine receptors. Pharmacol Rev 63:182-217
5. Ligresti G, Libra M, Militello L, Clementi S, Donia M, Imbesi R, Malaponte G, Cappellani A, McCubrey JA, Stivala F 2008 Breast cancer: Molecular basis and therapeutic strategies. Mol Med Rep 1:451-458
6. Murphy MB, Murray C, Shorten GD 2001 Fenoldopam: a selective peripheral dopamine-receptor agonist for the treatment of severe hypertension. N Engl J Med 345:1548-1557
7. Bodei S, Arrighi N, Spano P, Sigala S 2009 Should we be cautious on the use of commercially available antibodies to dopamine receptors? Naunyn Schmiedebergs Arch Pharmacol 379:413-415
8. Weber RR, McCoy CE, Ziemniak JA, Frederickson ED, Goldberg LI, Murphy MB 1988 Pharmacokinetic and pharmacodynamic properties of intravenous fenoldopam, a dopamine1-receptor agonist, in hypertensive patients. Br J Clin Pharmacol 25:17-21
9. Pennant M, Takwoingi Y, Pennant L, Davenport C, Fry-Smith A, Eisinga A, Andronis L, Arvanitis T, Deeks J, Hyde C 2010 A systematic review of positron emission tomography (PET) and positron emission tomography/computed tomography (PET/CT) for the diagnosis of breast cancer recurrence. Health Technol Assess 14:1-103
10. Chumpradit S, Kung MP, Billings JJ, Kung HF 1991 Synthesis and resolution of (+-)-7-chloro-8-hydroxy-1-(3'-iodophenyl)-3-methyl-2,3,4,5-tetrahydro- 1H-3- benzazepine (TISCH): a high affinity and selective iodinated ligand for CNS D1 dopamine receptor. J Med Chem 34:877-883

Oncogene (2015), 1–11

www.nature.com/onc

ORIGINAL ARTICLE

Expression and therapeutic targeting of dopamine receptor-1 (D1R) in breast cancer

DC Borcherding[1], W Tong[2], ER Hugo[1], DF Barnard[1], S Fox[1], K LaSance[3], E Shaughnessy[4] and N Ben-Jonathan[1]

Patients with advanced breast cancer often fail to respond to treatment, creating a need to develop novel biomarkers and effective therapeutics. Dopamine (DA) is a catecholamine that binds to five G protein-coupled receptors. We discovered expression of DA type-1 receptors (D1Rs) in breast cancer, thereby identifying these receptors as novel therapeutic targets in this disease. Strong to moderate immunoreactive D1R expression was found in 30% of 751 primary breast carcinomas, and was associated with larger tumors, higher tumor grades, node metastasis and shorter patient survival. DA and D1R agonists, signaling through the cGMP/protein kinase G (PKG) pathway, suppressed cell viability, inhibited invasion and induced apoptosis in multiple breast cancer cell lines. Fenoldopam, a peripheral D1R agonist that does not penetrate the brain, dramatically suppressed tumor growth in two mouse models with D1R-expressing xenografts by increasing both necrosis and apoptosis. D1R-expressing primary tumors and metastases in mice were detected by fluorescence imaging. In conclusion, D1R overexpression is associated with advanced breast cancer and poor prognosis. Activation of the D1R/cGMP/PKG pathway induces apoptosis *in vitro* and causes tumor shrinkage *in vivo*. Fenoldopam, which is FDA (Food and Drug Administration) approved to treat renal hypertension, could be repurposed as a novel therapeutic agent for patients with D1R-expressing tumors.

Oncogene advance online publication, 19 October 2015; doi:10.1038/onc.2015.369

INTRODUCTION

Dopamine (DA) is a catecholamine that acts as a major neurotransmitter in the brain and as a circulating hormone in the periphery, where it is produced by sympathetic nerves, adrenal medulla and gastrointestinal tract.[1] DA receptors (DARs) are expressed in kidney, gut and coronary arteries,[1,2] and their dysregulation is associated with hypertension, gut motility disorders and metabolic dysfunctions.[2–4] After discovering expression of functional DAR in human adipocytes and breast adipose tissue,[5] we questioned whether they are also expressed in breast cancer, and if so, what are their functions.

DA binds to five G protein-coupled membrane receptors (GPCRs), grouped by structure, pharmacology and function into DA type-1 receptor (D1R)-like (D1R and D5R) and D2R-like (D2R, D3R and D4R) receptors. According to the original classification, D1R-like receptors are coupled to Gαs proteins, activate adenylate cyclase (AC), increase cAMP and stimulate protein kinase A (PKA), while D2R-like receptors are coupled to Gαi/o proteins, inhibit AC, suppress cAMP and inhibit PKA.[6] Such classification is oversimplified, however, since DAR can couple to other G proteins and activate alternative signaling pathways such as the guanylate cyclase (GC)/cGMP/protein kinase G (PKG) pathway.[7,8]

Activation of D1R-like in striatal neurons,[9,10] coronary arteries[11] and adipocytes[5] increases cGMP, which is generated from GTP by two GCs: particulate (pGC) and soluble (sGC). The pGCs are activated by natriuretic peptides, while cytosolic sGCs are the main targets of nitric oxide (NO);[12] sGC can be directly stimulated by YC-1 and Riociguat.[13] Elevated cAMP or cGMP is rapidly hydrolyzed by phosphodiesterases (PDEs), a superfamily with 11 members that differ in substrate specificity and catalytic properties.[14] Viagra (Sildenafil), Cialis (Tadalafil) and Levitra (Vardenafil), used to treat erectile dysfunction, selectively inhibit PDE5 that hydrolyzes cGMP,[15] resulting in sustained cGMP elevation that can lead to apoptosis.[16] Cialis has the longest half-life of the PDE5 inhibitors.[17]

Dopaminergic drugs are widely used to treat Parkinson's disease, schizophrenia, addiction and hyperprolactinemia. Fenoldopam (Fen) is a high affinity (Kd = 2.3 nM) peripheral D1R agonist,[18] which does not activate D2R and does not penetrate the brain. Fen is FDA (Food and Drug Administration) approved to treat renal hypertension,[19] while causing only a small drop in blood pressure in normotensive patients.[20] Given its short half-life in the circulation,[21] Fen is commonly administered by infusion.

Our objectives were to (1) explore D1R expression in breast cancer cell lines and primary carcinomas, and examine for correlations with tumor attributes and disease outcome; (2) determine whether D1R activation induces apoptosis in breast cancer cells, and investigate the mechanism involved; (3) examine whether Fen suppresses tumor growth in mouse xenograft models; and (4) develop an imaging approach for visualizing D1R-expressing tumors and metastases.

RESULTS

D1R expression in breast carcinomas and cell lines

The *DRD1* transcript, cloned from MDA-MB-231 cells, was found identical to the published sequence. Breast carcinomas and matched normal breast tissue from the same individuals were analyzed for *DRD1* gene expression by RT–PCR (Figure 1a), and D1R proteins by western blotting (Figure 1b). *DRD1* expression

[1]Department of Cancer Biology, University of Cincinnati, Cincinnati, OH, USA; [2]Department of Pathology, University of Cincinnati, Cincinnati, OH, USA; [3]Department of Radiology, University of Cincinnati, Cincinnati, OH, USA and [4]Department of Surgery, University of Cincinnati, Cincinnati, OH, USA. Correspondence: Professor N Ben-Jonathan, Department of Cancer Biology, University of Cincinnati Medical College, 3125 Eden Avenue, Cincinnati, OH 45267 0521, USA.
E-mail: Nira.Ben-Jonathan@uc.edu
Received 17 March 2015; revised 31 July 2015; accepted 28 August 2015

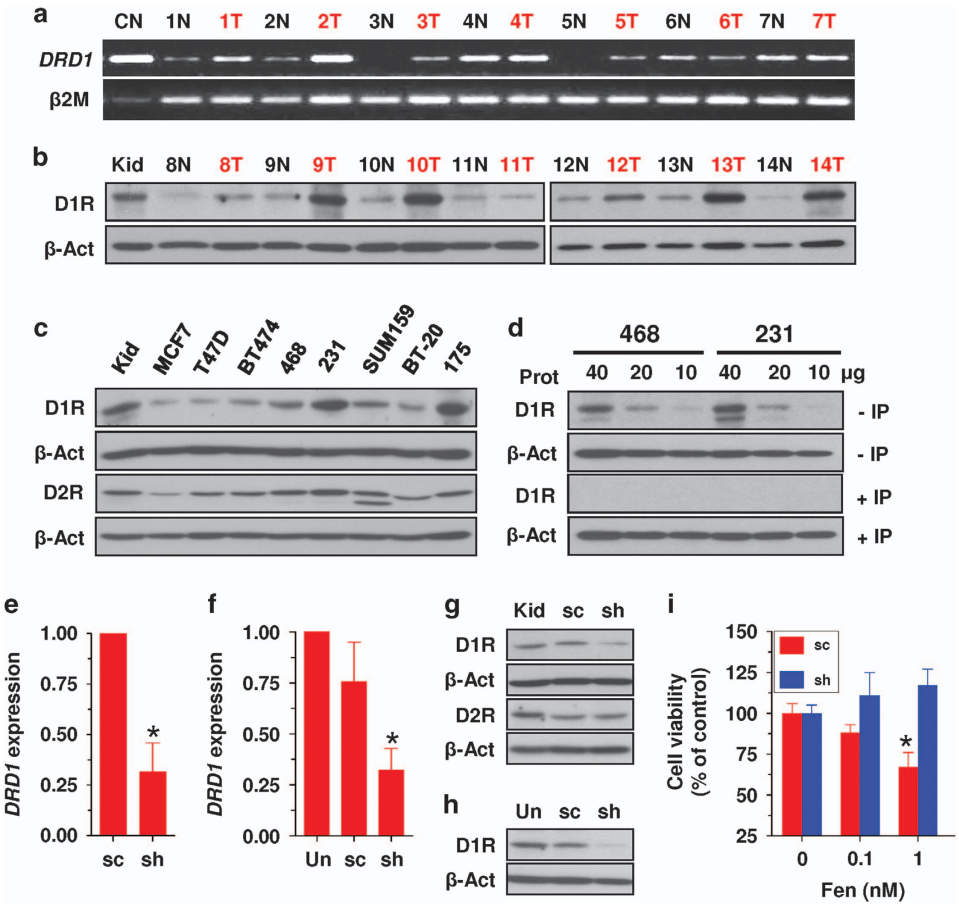

Figure 1. D1R expression in breast tumors and cell lines. *DRD1* gene (**a**) and protein (**b**) expression in tumors (T) and matching normal breast tissue (N), determined by RT–PCR and western blotting, respectively. CN, caudate nucleus; β2M, β2-microglobulin; Kid, kidney; β-Act, β-Actin. (**c**) D1R and D2R expression, determined by western blotting, in eight breast cancer cell lines. 468: MDA-MB-468, 231: MDA-MB-231, 175: MDA-MB-175. (**d**) Validation of the anti-D1R rabbit mAb. Blots were probed with untreated mAb (−IP), or with mAb pre-incubated with the immunizing peptide (+IP). (**e**) *DRD1* gene knockdown in MDA-MB-231 cells. *DRD1* gene expression was determined by qPCR in cells transiently transfected with scrambled (sc) or *DRD1* shRNA (sh) sequences. Data are presented as relative changes vs sc cells (means ± s.e.m., $n = 5$, $^*P < 0.01$). (**f**) *DRD1* gene expression was determined by qPCR in HEK293T cells that were either untransfected (Un) or transiently transfected with sc or sh sequences. Data are presented as relative changes vs Un cells (means ± s.e.m., $n = 3$, $^*P < 0.01$). Reduced D1R proteins, as determined by western blotting in MDA-MB-231 (**g**) and HEK293T (**h**) cells, transiently transfected with *DRD1* shRNA. Unchanged D2R protein levels are shown in (**g**). (**i**) *DRD1* knockdown in MDA-MB-231 cells abrogated the suppression of cell viability by Fenoldopam (Fen). Cells stably transfected with scrambled or *DRD1* shRNA sequences were incubated with Fen for 4 days and cell viability was analyzed by resazurin (means ± s.e.m., $n = 6$, $^*P < 0.05$). Gel images and graphs in this and subsequent figures are representative of at least three experiments.

was higher in tumors than in normal breast in 4/7 samples, while tumor D1R proteins were higher in 6/7 samples. Expression of D1R and D2R proteins was compared in eight breast cancer cell lines (Figure 1c). D1R proteins were most abundant in the triple-negative MDA-MB-231, SUM159 and MDA-MB-468 cells, and generally lower in the estrogen receptor (ER)-positive MCF7, T47D and BT474 cells, except for the ER-positive MDA-MB-175 cells. All cell lines also expressed variable levels of D2R (Figure 1c).

Given reports on lack of specificity of some antibodies against DAR,[22,23] we validated the rabbit anti-D1R monoclonal antibodies (mAb) used here. Antibody pre-absorption with the immunizing peptide abolished the D1R bands in cell lysates (Figure 1d). *DRD1* knockdown by short hairpin RNA (shRNA) in MDA-MB-231 cells (Figure 1e) and HEK293T cells (Figure 1f) markedly decreased the D1R protein band (Figures 1g and h, respectively); D1R knockdown did not affect D2R protein levels in MDA-MB-231 cells (Figure 1g). Fen did not suppress the viability of MDA-MB-231 cells with downregulated D1R (Figure 1i).

Immunohistochemistry (IHC) was used to visualize D1R in carcinomas and normal breast tissue. Figure 2a shows a carcinoma with strong D1R staining, which was eliminated by antibody pre-absorption with immunizing peptide (Figure 2b). A D1R-negative carcinoma and D1R-negative normal breast tissue are shown in Figures 2c and d, respectively.

Tissue microarrays (TMAs) were used to score 751 ductal breast carcinomas and 30 normal breast samples for D1R by IHC. Table 1 provides details of clinical data. Strong to intermediate D1R staining was seen in 29% of the tumors (Figure 2e), while 56% of tumors and all normal breast tissue samples were D1R negative. D1R staining was significantly associated with pre-menopausal age, ER-negative, progesterone receptor (PR)-negative, but Her2-overexpressing tumors (Table 2). A significant association was seen between D1R-positive tumors and higher tumor stage (Figure 2f), grade (Figure 2g) and node metastases (Figure 2h). A Kaplan–Meier analysis of 508 tumors revealed that patients with D1R-negative tumors had a median survival of 12 years, compared with 6 years for those with D1R-positive tumors (Figure 2i); recurrence-free survival was similarly shortened (Figure 2j). Supplementary Table 3 shows the statistical analyses.

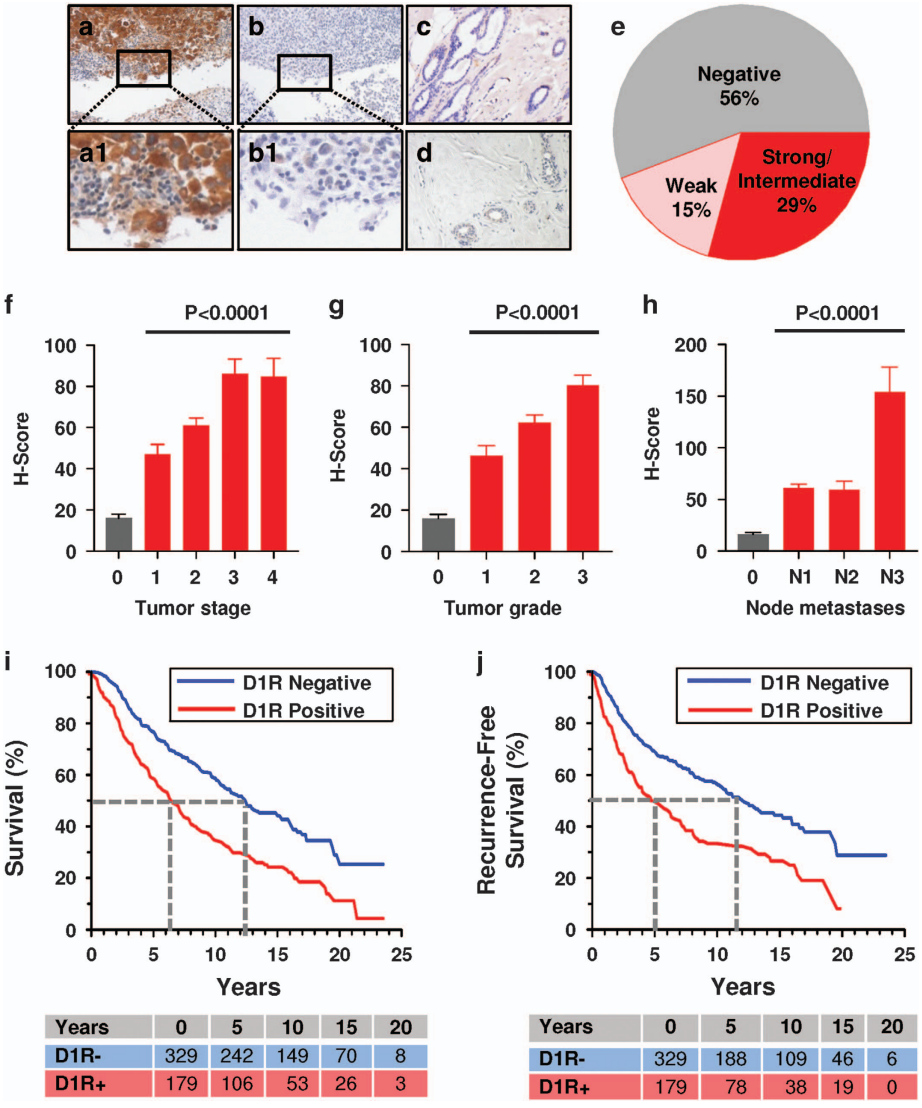

Years	0	5	10	15	20
D1R-	329	242	149	70	8
D1R+	179	106	53	26	3

Years	0	5	10	15	20
D1R-	329	188	109	46	6
D1R+	179	78	38	19	0

Figure 2. Immunoreactive D1R in breast carcinomas and associations with tumor attributes and patient survival. (**a**–**d**) Photomicrographs (×10) of D1R-positive carcinoma before (**a**) and after (**b**) mAb pre-absorption with the immunizing peptide. (**a1** and **b1**) × 10 of (**a**) and (**b**). (**c**) D1R-negative carcinoma. (**d**) D1R-negative normal breast tissue. (**e**) Distribution of immunoreactive D1R in TMAs with 751 breast carcinomas and 30 normal breast samples. Data shown are percent of total tumor number, using H-scoring; all 30 normal tissue samples were D1R-negative (H-score ⩽ 50). Positive D1R expression in carcinomas correlates with higher tumor stage (**f**), grade (**g**) and node metastasis (**h**); $P < 0.0001$. Positive D1R expression is associated with shorter patient survival (**i**), and recurrence-free survival (**j**), determined by Kaplan–Meier analysis of 508 tumors. The numbers of surviving or recurrence-free patients with D1R+ and D1R− tumors over a 20-year follow-up period are listed in the tables below the corresponding graphs. Supplementary Table 3 lists details of the Cox proportional hazards model for predictors of mortality.

Suppression of cell viability and induction of apoptosis

DA and three D1R agonists markedly suppressed viability of MDA-MB-231 and MDA-MB-468 cells, whereas cabergoline, a D2R agonist, had no effect (Figure 3a). DA and Fen caused a 25–50% suppression of BT-20 and SUM159 viability, were less effective in T47D cells and were ineffective in MCF7 cells (Figure 3b).

Reduced cell viability could be due to decreased proliferation and/or increased apoptosis. Since bromodeoxyuridine (BrdU) incorporation was unaltered by D1R activation (Figure 4d), we focused on apoptosis. Treatment of MDA-MB-231 cells with DA or D1R agonist (SKF38393) increased the percent of apoptotic cells twofold, as determined by flow cytometry (Figures 4a and b), while Fen increased terminal deoxynucleotidyl transferase-mediated dUTP nick-end labeling (TUNEL)-stained apoptotic cells fourfold (Figure 4c), and induced cleavage of caspase 9 (Figure 4e).

Inhibition of cell invasion

Boyden chambers were used to examine whether D1R activation affects FBS-induced cell invasion. As depicted in Figure 5a, incubation of MDA-MB-231 cells with DA or Fen inhibited FBS-stimulated invasion by 70%, with lower effects seen in BT-20 cells. Photomicrographs of invaded MDA-MB-231 cells are shown in Figure 5b.

Signaling through the cGMP/PKG pathway

Because D1R agonists are categorized as cAMP/PKA activators, we first examined their effects on cAMP. Unexpectedly, a 60-min incubation of MDA-MB-231 cells with 10 nM DA or Fen caused 25 and 50% decreases in cAMP, respectively (Figure 6a). Forskolin, a direct AC activator, induced a sixfold increase in cAMP, indicating an intact AC/cAMP machinery. In contrast, DA or Fen increased intracellular cGMP levels twofold, while Forskolin had no effects.

Table 1. Patient demographics and tumor data

Patient characteristics	*Patients no. (%)*
Age	
⩽55 years	386 (51)
>55 years	365 (49)
Tumor grade	
Grade I	121 (16)
Grade II	380 (51)
Grade III	250 (33)
Tumor stage	
T1	148 (20)
T2	377 (50)
T3	148 (20)
T4	78 (10)
Lymph node stage	
N0	272 (36)
N1	398 (53)
N2	71 (10)
N3	10 (1)
Metastasis stage	
M0	746 (99)
M1	5 (1)
Hormone status	
ER positive	463 (62)
PR positive	424 (56)
Her2 overexpressing	161 (21)
Triple negative	143 (19)
D1R stain results	
Negative	420 (56)
Weak positive	113 (15)
Intermediate positive	163 (22)
Strong positive	55 (7)

Abbreviations: D1R, dopamine type-1 receptor; ER, estrogen receptor; PR, progesterone receptor.

Table 2. Correlation of D1R staining and tumor characteristics

Clinical data	*No. of patients*	*D1R positive no. (%)*	*P-value (chi^2)*
All	751	331 (44)	
Age			
⩽55 years	386	187 (48)	0.001
>55 years	365	144 (39)	
Tumor size			
⩽2 cm	148	46 (31)	
2–5 cm	377	159 (42)	
>5 cm	226	126 (56)	<0.0001
Lymph node stage			
N0	272	124 (46)	
N1	398	169 (42)	
N2	71	28 (39)	
N3	10	10 (100)	<0.0001
Tumor grade			
Grade I	121	40 (33)	
Grade II	380	161 (42)	
Grade III	250	130 (52)	0.0004
ER positive			
Yes	463	182 (39)	
No	288	150 (52)	<0.0001
PR positive			
Yes	424	173 (41)	
No	327	161 (49)	0.02
Her2 overexpressing			
Yes	161	84 (52)	0.01
No	590	249 (42)	
Triple negative			
Yes	143	72 (50)	0.06
No	608	264 (43)	

Abbreviations: D1R, dopamine type-1 receptor; ER, estrogen receptor; PR, progesterone receptor.

We reasoned that if D1R activation reduces cell viability by increasing cGMP, bypassing the receptor and directly stimulating cGMP should have similar effects. Indeed, Figure 6b shows that YC-1, a direct sGC stimulator, reduced cell viability to 5–25% of controls, whereas KT5823, a selective PKG inhibitor, prevented Fen-induced apoptosis (Figure 6c), confirming mediation of apoptosis by PKG. Cialis, which blocks PDE5 and prolongs cGMP elevation, moderately suppressed cell viability when used alone, but markedly enhanced Fen-induced apoptosis to 15% of controls (Figure 6d). Other signaling pathways, for example, ERK1/2, Akt and CREB, were differentially activated by Fen (Supplementary Figure S1). To verify that DA inhibits cell viability via D1R, cells were pretreated with the D1R antagonist SCH39166. Figure 6e confirms that D1R blockade abrogated DA-induced suppression of cell viability.

Fenoldopam markedly inhibits growth of xenografts

Two mouse xenograft models were used to examine the *in vivo* effects of Fen on tumor growth. In one model, mice were inoculated with MDA-MB-231 cells into the inguinal mammary fatpad. When tumor volumes reached ~250 mm^3, Alzet osmotic mini-pumps containing vehicle, high-dose (calculated to generate serum levels of ~30 nM) or low-dose (10 nM) Fen, were implanted subcutaneously. Within 1 week, Fen at high dose significantly reduced tumor volume (Figure 7a). After 3 weeks, tumor volumes in mice treated with high- and low-dose Fen were 40 and 60% of controls, respectively. None of these mice showed adverse physical or behavioral effects. After 3 weeks, tumors treated with high-dose Fen were half the weight of controls (Figure 7d), showed a fourfold increase in apoptosis (Figure 7e), and a twofold increase in necrosis (Figure 7f).

Other mice were inoculated in the flank with SUM159 cells, and high-dose Fen was delivered by Alzet pumps as above. Compared with the robust growth of control tumors, Fen caused a dramatic suppression of tumor volumes (Figure 7g) and weights (Figure 7h) to 15% of controls. Remarkably, when pumps were removed after 1 week, tumor growth remained suppressed for at least 2 more weeks (Figure 7g).

In vivo imaging of D1R-expressing tumors

We also developed *in vivo* imaging for detecting D1R-expressing tumors. Mice with MDA-MB-231-derived tumors were intravenously injected with rabbit anti-D1R mAb conjugated to Alexa-Fluor 647 fluorescent dye. Figure 7c shows fluorescence imaging 24 h after the injection. One mouse shows intense fluorescence at the primary tumor, while another also has fluorescence in distal metastases, as confirmed histologically (Figure 7c).

Figure 8 presents our working model. D1R activation by agonists such as Fen, stimulation of sGC by YC-1, and PDE5 blockade by Cialis, all increase cGMP levels, which stimulate PKG.

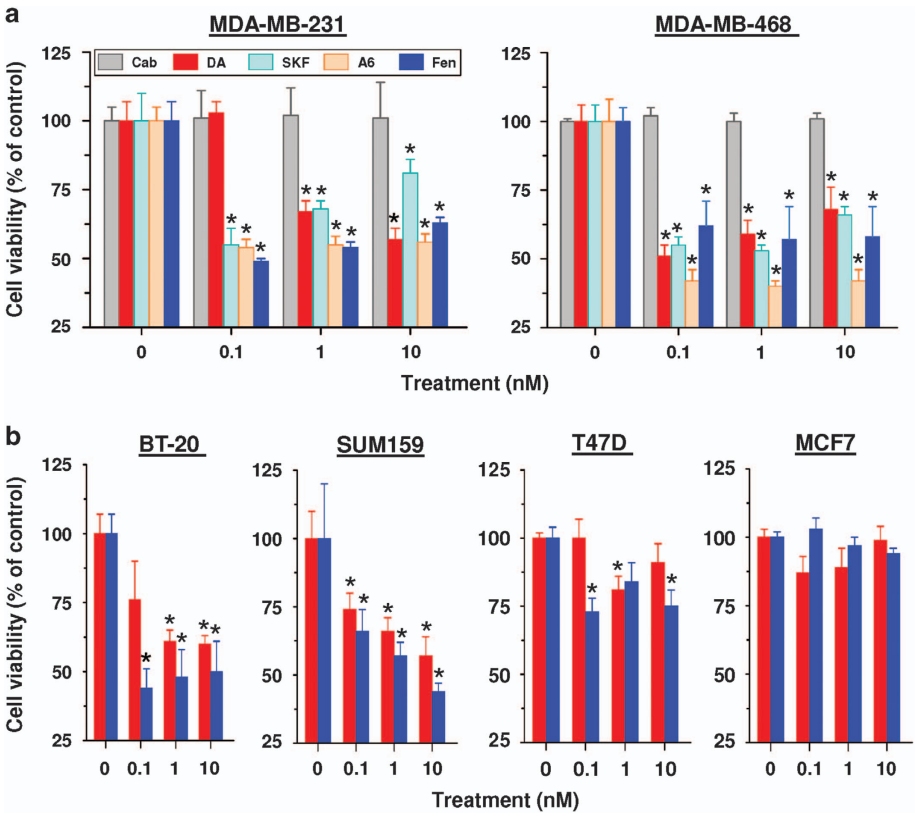

Figure 3. DA and D1R agonists, but not a D2R agonist, reduced the viability of multiple breast cancer cells. (**a**) MDA-MB-231 and MDA-MB-468 cells were incubated for 4 days with increasing concentrations of DA, cabergoline (Cab), a D2R agonist, or three D1R agonists: SKF38393 (SKF), A68930 (A6) or Fenoldopam (Fen). Cell viability was determined by a resazurin assay (means ± s.e.m., $n = 6$, $^*P < 0.05$). (**b**), BT-20, SUM159, T47D and MCF7 cells were incubated with increasing concentrations of DA or Fen. Experimental details and statistical analyses are the same as in (**a**).

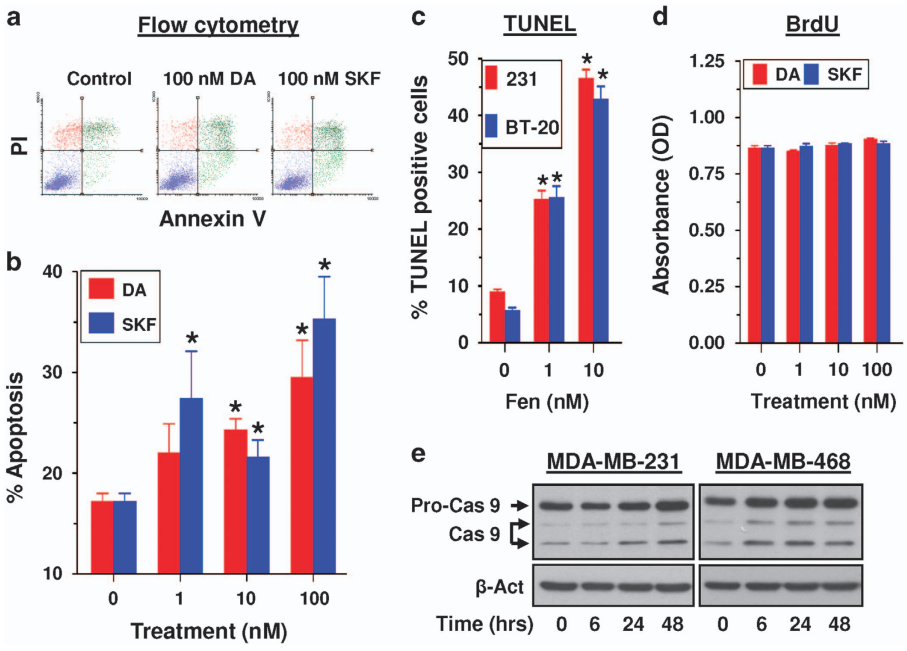

Figure 4. DA and D1R agonists induce apoptosis and inhibit cell invasion. (**a**, **b**) Induction of apoptosis by DA and SKF38393 (SKF), incubated with MDA-MB-231 cells for 48 h, as determined by Annexin V/Propidium Iodide staining followed by flow cytometry. (**c**) Treatment of MDA-MB-231 and BT-20 cells with Fen for 48 h increased apoptosis, as determined by TUNEL staining. Results are presented as percent of TUNEL-positive cells ($^*P < 0.05$). (**d**) DA and SKF did not affect cell proliferation. MDA-MB-231 cells were incubated with the ligands for 48 h and BrdU incorporation was determined by an ELISA (means ± s.e.m., $n = 4$, $^*P < 0.05$). (**e**) Cleavage of caspase 9 in MDA-MB-231 and MDA-MB-468 cells treated with 1 nM Fen for the indicated times. The upper band is pro-caspase 9, while the lower two bands are its cleavage products.

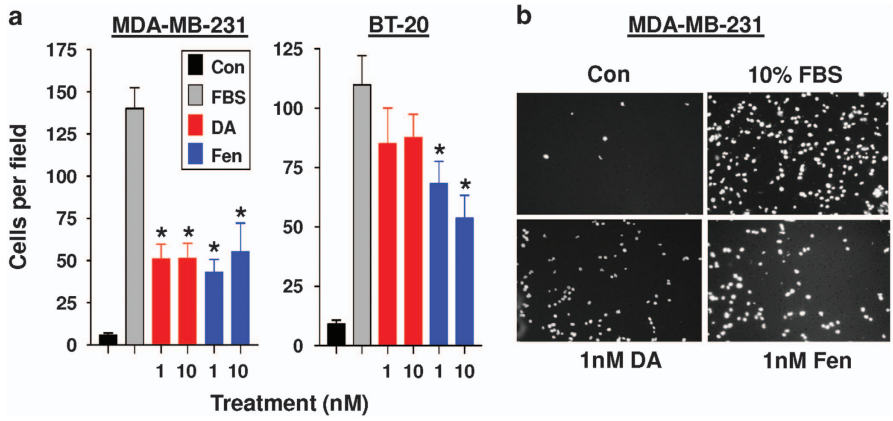

Figure 5. Inhibition of FBS-induced cell invasion by DA and Fenoldopam (Fen). (**a**) Treatment of MDA-MB-231 and BT-20 cells with DA or Fen for 24 h reduced FBS-induced cell invasion through Matrigel-coated Boyden chambers. Serum-free medium served as a control, and 10% FBS served as a chemoattractant. Cells on the membrane underside, stained with Hoechst dye, were photographed and counted (means ± s.e.m., $n = 3$, $^*P < 0.05$). (**b**) Representative photographs of invaded MDA-MB-231 cells.

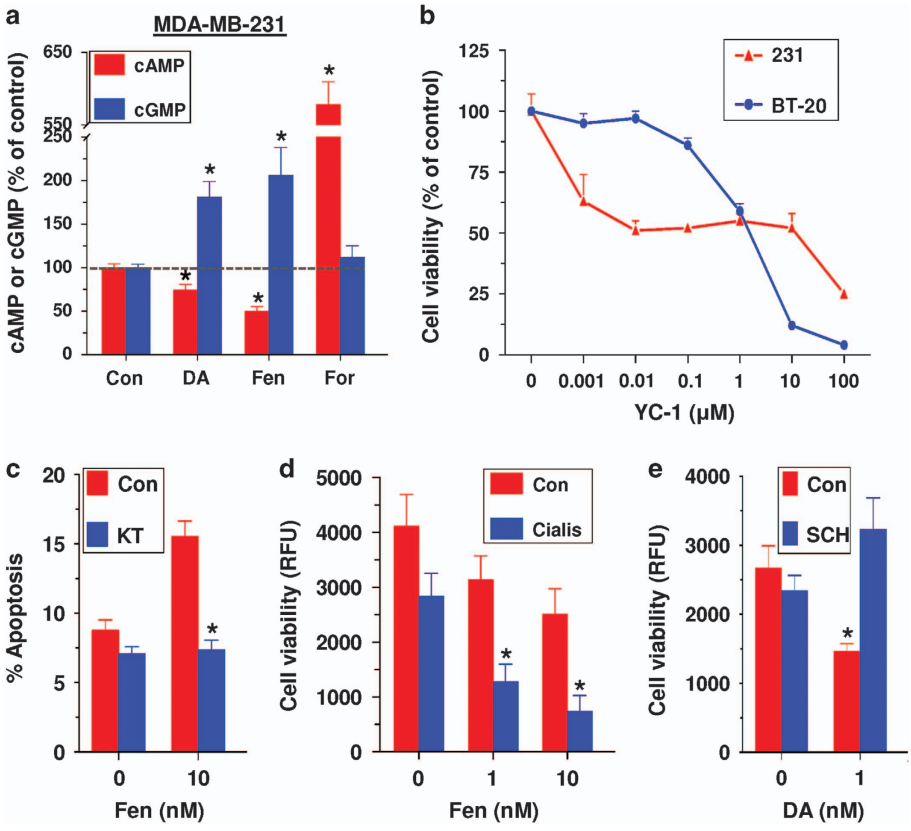

Figure 6. Activation of the cGMP/PKG signaling pathway by DA and Fen. (**a**) Suppression of cAMP and stimulation of cGMP in MDA-MB-231 cells incubated with 10 nM DA or Fen for 60 min; Forskolin (10 μM) served as a positive control for cAMP (means ± s.e.m., $n = 6$, $^*P < 0.05$). (**b**) YC-1, a sGC activator, suppressed MDA-MB-231 and BT-20 cell viability (means ± s.e.m., $n = 6$). (**c**) KT5823 (KT), a PKG inhibitor, abrogated Fen-induced apoptosis. MDA-MB-231 cells were pre-incubated with 5 μM KT for 30 min, followed by incubation with 10 nM Fen for 48 h; apoptosis was determined by TUNEL (means ± s.e.m., $n = 4$, $^*P < 0.05$). (**d**) Cialis (1 μM), a PDE5 inhibitor, inhibited the viability of SUM159 cells, incubated with or without Fen for 4 days (means ± s.e.m., $n = 6$, $^*P < 0.05$). (**e**) SCH39166 (SCH), a D1R antagonist, abrogated DA-induced inhibition of cell viability (means ± s.e.m., $n = 4$, $^*P < 0.05$).

Activated PKG increases apoptosis and suppresses invasion. A functional link between D1R and sGC may involve inducible nitric oxide synthase, which generates the second messenger NO.[24]

DISCUSSION

This study reports three major findings: (1) substantial expression of D1R in human breast carcinomas and cell lines, (2) induction of apoptosis by D1R activation via the cGMP/PKG signaling pathway and (3) profound suppression of tumor growth by Fen, a peripheral D1R agonist. Nearly one-third of 751 breast carcinomas had strong to moderate D1R staining, while normal breast samples were D1R negative. There was significant correlation between immunoreactive D1R and advanced disease, that is, tumors of higher stage, grade and lymph node metastases. Notably, positive D1R staining was associated with ER-negative,

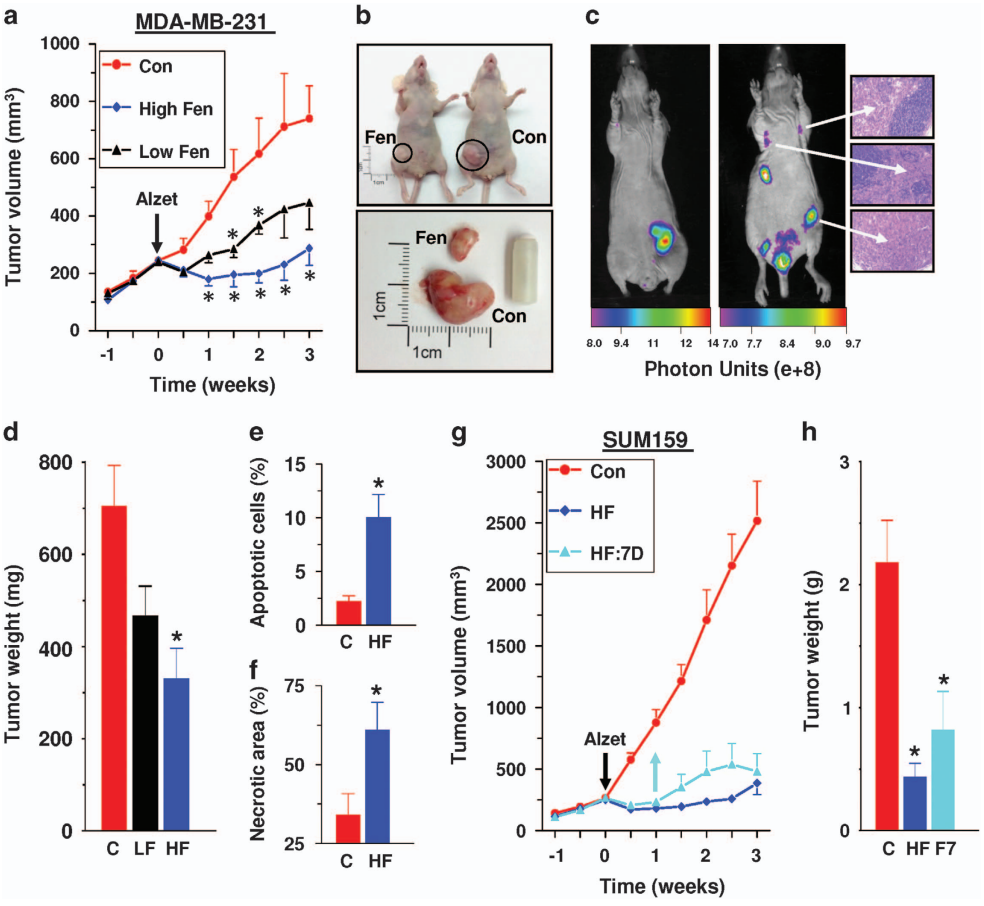

Figure 7. Fenoldopam Inhibits tumor growth in two mouse xenograft models. (**a**) Fen suppresses growth of orthotopic MDA-MB-231 xenografts. Mice were implanted with Alzet pumps delivering vehicle (Con), high Fen (400 ng/kg/min) or low Fen (133 ng/kg/min) for 3 weeks (means ± s.e.m., $n = 7$–8 mice, $*P < 0.05$). (**b**) Mice with control- and high Fen-treated tumors, and the same tumors, pictured with an Alzet pump, removed after 3 weeks. (**c**) Mice with MDA-MB-231-derived tumors were intravenously injected with human anti-D1R antibody conjugated to Alexa-Fluor 647. *In vivo* fluorescence imaging after 24 h shows intense fluorescence of the primary tumors and metastases. Arrows indicate insets of H&E staining of the primary tumor and metastases in the axillary lymph nodes. Injection of rabbit IgG conjugated to Alexa-Fluor 647 produced no fluorescence (not shown). Fen treatment for 3 weeks decreased the weight of MDA-MB-231-derived tumors (**d**), increased TUNEL-positive apoptotic cells (**e**) and augmented necrosis (**f**). (**g**) Treatment with high Fen markedly reduced growth of SUM159-derived xenografts inoculated in the flank. One group (HF) had the pumps for 3 weeks, while another (HF:7D), had the pumps removed after 1 week (means ± s.e.m., $n = 6$–8 mice). All time points in the two groups were lower than controls ($P < 0.05$). (**h**) SUM159-derived tumor weights 3 weeks after Alzet implantation ($*P < 0.05$).

PR-negative, but with Her2/neu-overexpressing tumors, indicating that D1R-expressing tumors do not fit within the 'triple negative' category. Most importantly, D1R expression predicts poor prognosis, as indicated by a shorter patient survival.

These data suggest that D1R is a novel prognostic biomarker in advanced breast cancer. D1R expression can be detected in tumor biopsies by IHC, or by non-invasive imaging such as positron emission tomography, using radioactive D1R-selective ligands.[25,26] We foresee that many patients could benefit from targeted D1R therapy. FDA-approved drugs such as Fenoldopam, Riociguat, a sGC activator,[27] and Cialis, a PDE5 inhibitor, could be repurposed for treating breast cancer patients with advanced disease who do not respond to standard treatments.

Expression of DAR in peripheral tissues and in some cancers has been reported,[2] but there is only scant information on their expression in breast cancer. A small study reported binding of [H^3] spiperone, a D2R-like antagonist, in breast tumors,[28] and a recent study described D3R and D5R expression in breast cancer stem cells.[29] However, there are no reports on specific detection of D1R expression in human tumors outside the brain. Nonetheless, an epidemiological study found an association between DAR antagonists (that is, antipsychotics and anti-emetics) and a small increase in breast cancer risk.[30]

DA and three D1R agonists suppressed cell viability, inhibited invasion and induced apoptosis in multiple breast cancer cell lines, while a D2R agonist was ineffective. Others reported that DA or its agonists induce apoptosis in neuroblastoma,[31] leukemia,[29] ovarian,[32] breast[29,33,34] and colon[33] cancer cells. However, most studies did not identify which DAR was expressed in their samples, and often used DA or its agonists at high pharmacological doses, raising the possibility of toxic effects. In contrast, we have confirmed expression of both D1R gene and protein in breast cancer cell lines and primary carcinomas, and demonstrated that selective D1R agonists *at low* nM *doses* suppress cell viability and induce apoptosis. Because *DRD1* has no introns, our studies carefully verified lack of genomic DNA contamination and we also validated the specificity of the anti-D1R antibodies.

It appears counterintuitive that increased D1R expression correlates with advanced disease while D1R activation, rather than its suppression, results in apoptosis. This enigma raises several questions: (a) Is the *DRD1* gene coincidentally upregulated in tumors because of proximity to an overexpressed oncogene in

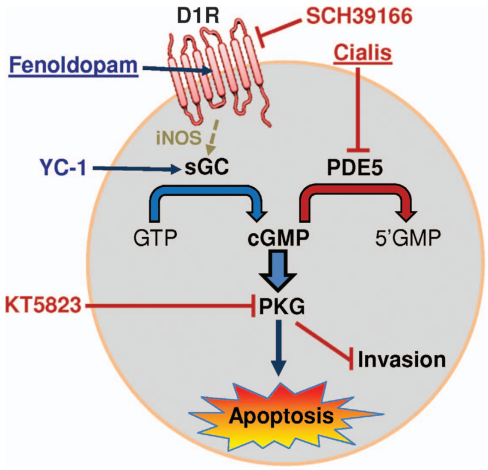

Figure 8. Proposed model of D1R signaling via the cGMP/PKG pathway in breast cancer cells. Fen binds to D1R, activates sGC, increases cGMP levels and activates PKG. This culminates in increased apoptosis and decreased invasion. This pathway can also be activated by YC-1 through sGC, and by Cialis, through a blockade of PDE5. SCH39166 is a selective D1R antagonist while KT5823 is a selective PKG antagonist. Inducible nitric oxide synthase (iNOS) may mediate the activation of sGC by D1R. FDA-approved drugs for various diseases are underlined.

breast carcinomas?, (b) Does D1R have ligand-independent actions as is the case for Her-2?, (c) Does D1R heterodimerize with another DAR or with other GPCRs?,[35] (d) Is the functional link between D1R and the cGMP apoptotic pathway being maintained or is lost during tumor progression?, (e) What is the minimal level of D1R expression which is necessary for responsiveness to a ligand? and (f) Does D1R have a different role during initiation, progression and/or metastatic stages of the disease? These questions should be addressed in future investigations.

Another issue is whether circulating DA alters growth of DAR-expressing tumors. Free DA circulates at very low levels, well below its Kd values. However, most DA in humans circulates as DA-sulfate (DA-S), at 10-fold higher basal serum levels than all free catecholamines combined.[36] Sulfo-conjugation of DA, which is done in the gut by SULT1A3, is the major form of peripheral DA inactivation in humans, while glucuronidation predominates in rodents.[37] DA-S does not bind DAR and is biologically inactive. However, unlike irreversible DA inactivation by deamination, O-methylation or glucuronidation, sulfoconjugation is reversed by arylsulfatase A, a releasable lysosomal enzyme.[38]

Based on our discovery that human adipocytes express arylsulfatase A which converts DA-S to bioactive DA,[5] we postulate that DAR-expressing breast tumors respond to serum DA-S only if they have an active arylsulfatase A. Moreover, stimulation vs inhibition of tumor growth by circulating DA-S/DA depends on a balance of D1R-like and D2R-like expression in each tumor. Because Fen at low nM levels is highly selective for D1R, its ability to suppress D1R-expressing tumors should not be compromised by the presence of D2R-like. Notably, rodents do not have a SULT1A3 ortholog,[39] and have very low serum-free DA levels and no DA-S. Consequently, mice carrying human cancer xenografts are not good models for assessing whether serum DA-S/DA affects tumor growth in humans. Also, a proper response to agonists requires not only functional D1R, but also a coordinated action of all the components of the cGMP pathway (sGC, cGMP, PDE5 and PKG), which may differ among cell lines.

Our data show that D1R in breast cancer cells signals via the cGMP/PKG pathway, as reported for striatal neurons[9,10] and adipocytes.[5] Although D1R is classified by their ability to increase cAMP, we found a decrease, rather than an increase, in cAMP levels following D1R activation. This decrease may be secondary to elevated cGMP, which activates cAMP-hydrolyzing PDEs, underlying reciprocal relationships between the two cyclic nucleotides.[40] Striatal DA can signal through D1R to increase NO synthesis from L-arginine by activating neuronal NO synthase.[41,42] Elevated NO levels lead to sGC activation, increased cGMP accumulation and PKG activation, which often result in apoptosis.[43] Future studies should examine the mode of coupling of D1R to sGC, and determine whether NO is an upstream component of the D1R/sGC/cGMP/PKG signaling pathway in breast cancer.

A combination of apoptosis and necrosis is likely responsible for the more robust effects of Fen *in vivo* than *in vitro*. Tumor necrosis could be due to activation of multiple pathways within tumor cells, some of which can suppress angiogenesis.[44] DA has been reported to inhibit angiogenesis *in vivo* by acting via D2R[32,45,46] by inhibiting vascular endothelial growth factor[47] and its receptor.[48] However, there is no evidence that Fen at the low nM levels used in this study binds to D2R and directly affects angiogenesis. The long-lasting effects of Fen after termination of infusion, together with a future development of slow release formulation of orally-deliverable Fen, bode well for its prospective benefits in the treatment of patients with D1R-expressing tumors.

MATERIALS AND METHODS

Cell culture

MDA-MB-231, MDA-MB-468, MDA-MB-175-VII, BT-20, MCF-7, T47D, BT-474 and HEK293T were obtained from American Type Culture Collection (ATCC, Manassas, VA, USA); SUM159 cells were a gift from Dr S Wang (University of Cincinnati). All cell lines were authenticated by the RTSF Genomics Core (Michigan State University, East Lansing, MI, USA) and were routinely tested for mycoplasma contamination. Cells were cultured in DMEM, RPMI or DMEM/F12 (Corning, Corning, NY, USA) with 10% FBS (Atlanta Biologicals, Flowery Branch, GA, USA) and 50 μg/ml normocin (Invivogen, San Diego, CA, USA). Medium for T47D cells was supplemented with 1 μM insulin (Sigma, St Louis, MO, USA). Medium for BT-20 and MDA-MB-175-VII cells included 1% ITS+ premix (Corning). For all experiments, cells were plated in growth medium, followed by starvation in treatment medium containing 5% charcoal-stripped serum (Atlanta Biologicals) and 1 mM ascorbic acid (Sigma). After 24 h, cells were treated as indicated.

DRD1 cloning from breast cancer cell lines

Total RNA was isolated using RNAspin isolation kit (GE Healthcare, Pittsburgh, PA, USA). Oligo dT-primed cDNA was synthesized using SuperScript II (Invitrogen, Carlsbad, CA, USA). A subset of the *DRD1* transcript sequence, spanning a portion of the 5′ UTR, the entire protein coding sequence and a portion of the 3′ UTR (nucleotides 434–2316 of GenBank RefSeq NM_000794; Supplementary Table 1) was PCR amplified, using high fidelity Phusion DNA polymerase (Thermo Fisher Scientific, Pittsburgh, PA, USA) and cloned. *DRD1* sequences were successfully isolated from MDA-MB-231, MDA-MB-468 and MCF-7 cell lines, and sequenced by Genewiz (South Plainfield, NJ, USA). The MDA-MB-231 sequence was confirmed by a complete sequencing of both strands and shared 100% identity with the published sequence.

Conventional RT–PCR and quantitative real-time PCR

cDNA was synthesized from total RNA, using RT^2 HT First Strand Kit (Qiagen, Germantown, MD, USA). Because *DRD1* does not contain introns, DNase was added during RNA isolation and cDNA synthesis, and samples were evaluated for genomic DNA contamination by omitting reverse transcriptase. PCR amplification was done with primers for *DRD1,* or with intron-spanning primers for β2-Microglobulin (Supplementary Table 1). For conventional RT–PCR, products were resolved on 1.5% agarose gel and photographed. Quantitative real-time PCR (qPCR) was done using SYBR Green, and products were detected with a StepOnePlus instrument (Applied Biosystems, Carlsbad, CA, USA). Product purity was verified using DNA melting curve analysis and agarose gel electrophoresis. PCR efficiency was determined by the LinRegPCR program. Fold changes in

gene expression were calculated from cycle threshold and efficiency measurements.

Western blot analysis

Cells and tissue lysates (40 μg/sample) were separated on 12% SDS gels and transferred onto PDVF membranes. After overnight incubation with primary antibodies (Supplementary Table 2), followed by horseradish peroxidase-conjugated secondary antibodies, products were exposed to SuperSignal chemiluminescence reagents (Pierce, Rockford, IL, USA) and photographed. β-Actin was a loading control. For antibody validation, the rabbit anti-D1R mAb was incubated for 10 min with the immunizing peptide, matching the human D1R C-terminus sequence (Novus, NBP1-79050PEP, Novus, Littleton, CO, USA), before incubation with blots.

Knockdown of *DRD1* expression

A shRNA vector against human *DRD1* (MISSION shRNA SHCLND-NM_000794; TRCN0000011334, Sigma) was used to knockdown *DRD1* gene expression; scrambled vector (Sigma) was a negative control. Cells were transfected using Lipofectamine 2000 (Invitrogen). Knockdown was confirmed by qPCR and western blotting. For stable transfections, cells were selected using 0.5 μg/ml puromycin (Invivogen), and positive colonies were expanded.

Tissue samples

Matched frozen tissue or formalin-fixed paraffin-embedded (FFPE) slides of breast carcinomas and normal breast tissues were obtained from the University of Cincinnati Pathology Department. The institutional review board approved the use of de-identified samples; informed consent was obtained from all patients. TMAs containing FFPE samples of breast carcinomas and normal breast tissues were purchased from Lifespan Biosciences (Seattle, WA, USA, LS-SBRCA121, $n=60$), Biochain (Newark, CA, USA, Z7020005, $n=63$; Z7020008, $n=53$), Protein Biotechnologies (Ramona, CA, USA, TMA-1007, $n=67$), NCI Cancer Diagnosis Program (CDP) (stage II ($n=340$) or III ($n=168$) prognostic TMAs). A total of 751 primary ductal carcinomas and 30 normal breast tissues were analyzed for D1R expression by IHC. Samples with known outcome (508) were used for Kaplan–Meier analysis of overall patient survival and recurrence-free survival.

Immunohistochemistry

Antigen retrieval was done in boiling sodium citrate buffer for 12 min. Non-specific antibody binding was blocked, and slides were incubated with anti-D1R mAb (1:500), followed by anti-rabbit horseradish peroxidase-conjugated secondary antibody (1:500). Diaminobenzidine (DAB) was the chromogen, with hematoxylin counter-staining.

Scoring of IHC

IHC staining was scored by two investigators blinded to patient data. The histo-score (H-score) was calculated as intensity score (0 = none, 1 = weak, 2 = mild, 3 = moderate, 4 = strong) multiplied by percentage of stain-positive tumor cells ($\leqslant 50$ = negative, 51–100 = weak positive, 101–200 = intermediate positive, >200 = strong positive).

IHC statistics

H-score results were averaged between duplicate samples and the two observers. ANOVA was performed for comparing H-score with tumor stage, grade and node metastases. *P*-values <0.05 were considered as significant, and those with significance were adjusted by the Bonferroni method. Data were divided into positive (H-score >50) and negative (H-score $\leqslant 50$) staining groups, and Pearson's chi-square analysis was used to test for independence across different tumor characteristics. A multivariate Cox proportional hazards model was used for predictors of mortality. Kaplan–Meier analysis was used for association between D1R-positive or D1R-negative tumors and patient survival and recurrence-free survival. All statistical analyses were done using JMP version 10 (SAS Institute, Cary, NC, USA).

Cell viability assay

Cells plated at 5000 cells/well in 96-well plates were treated with DA, YC-1 (Sigma), Fen, SKF 38393, A68930, cabergoline (all from Tocris, Minneapolis, MN, USA), KT5823 (Cayman Chemical, Ann Arbor, MI, USA) or Cialis (Selleckchem, Houston, TX, USA). After 4 days, cell viability was determined by the resazurin fluorescence assay (Sigma).

Invasion assay

Cells were plated at 50 000 cells/well in serum-free medium on BioCoat Matrigel-coated inserts with 8 μm pore membranes (BD Biosciences, San Jose, CA, USA). Inserts were suspended over wells containing serum-free medium (Control), or medium with 10% FBS as chemoattractant with and without DA or Fen. After 24 h, non-invading cells were removed, and invading cells were stained with Hoechst fluorescent dye and Photographed at $\times 10$ magnification (Zeiss Axioplan Imaging 2 microscope, Zeiss, Thornwood, NY, USA), and cell number per field was counted in a blinded manner. Experiments included three inserts per treatment, with six random fields photographed per insert.

Flow cytometry

Cells plated at 200 000 cells/well in 6-well plates were treated for 48 h with drugs. Apoptosis was determined using FITC Annexin V Apoptosis Detection Kit 1 (556547; BD Pharmingen), and analyzed by flow cytometry using a Cell Lab Quanta SC Flow Cytometer (Beckman Coulter, Indianapolis, IN, USA). About 10 000 gated events were collected per treatment. Results were calculated using the Mod-fit program (Topsham, ME, USA).

TUNEL assay

Cells plated in 8-well chamber slides at 10 000 cells/well were incubated with drugs for 48 h, and formalin-fixed. FFPE tumors from mice were sectioned onto slides. Apoptotic cells were detected by TUNEL, using TACS TdT *In Situ* Apoptosis Detection Kit: DAB (R&D systems, Minneapolis, MN, USA), with hematoxylin counterstain. The number of TUNEL-positive cells was determined by counting four fields/treatment, and apoptosis was calculated as the number of apoptotic cells/total number of cells $\times 100$.

BrdU incorporation

Cells plated at 5000 cells/well in 96-well plates were treated with drugs for 48 h. BrdU incorporation was determined by ELISA cell proliferation kit (Roche, Indianapolis, IN, USA) and absorbance was determined on a KC Junior Plate Reader. Experiments included six replicates per treatment, and were repeated at least twice.

cGMP and cAMP analyses

Cells plated at 100 000 cells/well in 24-well plates were treated for 60 min. Lysates were analyzed for cAMP or cGMP using respective colorimetric competitive ELISA kits (Cayman Chemical; cAMP: 581001, cGMP: 581021). Limits of detection were 0.3 pmol/ml (cAMP) and 0.23 pmol/ml (cGMP).

Animals

Eight-week-old female athymic *nu/nu* mice were obtained from the NCI. Mice were housed four/cage in sterile cages, kept under light/dark cycles (12 h:12 h), and were acclimated for 7–10 days before experiments. The protocol (#04-06-29-01) was approved by the University of Cincinnati Institutional Animal Care and Use Committee.

Mouse xenograft models

MDA-MB-231 cells (1.5×10^6 cells/60 μl) or SUM159 cells (1×10^6cells/60 μl) were suspended 1:1 in PBS/Matrigel and inoculated into the inguinal mammary fatpad or subcutaneously in the flank, respectively. Tumor dimensions were measured twice/week and tumor volume calculated as length $\times$ width$^2\times0.52$. Power calculation, based on previous studies in our laboratory and those in the literature, predicts a 90% chance of finding significant differences ($\alpha=0.05$, power of 0.8) when using eight mice/treatment. Mice that were killed due to health issues were excluded. Mice were randomized among treatments. When tumors were 200–250 mm^3 in volume, Alzet osmotic mini-pumps (model 1004, Durect Corporation, Cupertino, CA, USA) with a 100-μl reservoir, rated for a continuous delivery at 0.11 μl/h for 4 weeks, were implanted subcutaneously in the dorsal neck. The pumps delivered PBS (control), high Fen (400 ng/kg/min) or low Fen (133 ng/kg/min). After 3 weeks, animals were killed and tumors were weighed. Tumors were FFPE for TUNEL assay or histopathology. One group

with SUM159-derived tumors had the pumps removed after 1 week and tumor monitoring continued for another 2 weeks.

In vivo fluorescence imaging

Rabbit anti-D1R mAb were fluorescently labeled using a SAIVI Alexa Fluor 647 Antibody Labeling Kit (Molecular Probes by Life Technologies). These antibodies (100 μg proteins) were injected via tail vein into mice with MDA-MB-231-derived inguinal tumors of moderate size. Mice were imaged 24 h after the injection, using Kodak Multispectral Imaging FX (Carestream Molecular Imaging). Rabbit IgGs labeled with Alexa Fluor 647 and injected into mice showed no specific fluorescence in the tumors.

Statistics

Number of replicates for each experiment with cultured cells was determined by the plate layout. Student's *t*-test or ANOVA was used where appropriate. *P*-values $\leqslant 0.05$ were considered as significant. All experiments were repeated at least three times, unless otherwise noted.

CONFLICT OF INTEREST

The authors declare no conflict of interest.

ACKNOWLEDGEMENTS

We dedicate this manuscript to Wilson Tong, M.D., whose untimely death was a major loss to all who knew him. We thank Dean Quaranta for technical assistance, and Drs Susan Waltz and Peter Stambrook for critical reviews of this manuscript. This investigation was funded by NIH grants CA096613 and ES020909, DOD grants AR110050 and BC122992, and pilot grants from Marlene Harris-Ride Cincinnati, and the University of Cincinnati Center for Clinical and Translational Science and Training (CCTST).

REFERENCES

1 Amenta F, Ricci A, Tayebati SK, Zaccheo D. The peripheral dopaminergic system: morphological analysis, functional and clinical applications. *Ital J Anat Embryol* 2002; **107**: 145–167.
2 Rubi B, Maechler P. Minireview: new roles for peripheral dopamine on metabolic control and tumor growth: let's seek the balance. *Endocrinology* 2010; **151**: 5570–5581.
3 Contreras F, Fouillioux C, Bolívar A, Simonovis N, Hernández-Hernández R, Armas-Hernandez MJ *et al*. Dopamine, hypertension and obesity. *J Hum Hypertens* 2002; **16**: S13–S17.
4 Li ZS, Schmauss C, Cuenca A, Ratcliffe E, Gershon MD. Physiological modulation of intestinal motility by enteric dopaminergic neurons and the D2 receptor: analysis of dopamine receptor expression, location, development, and function in wild-type and knock-out mice. *J Neurosci* 2006; **26**: 2798–2807.
5 Borcherding DC, Hugo ER, Idelman G, De Silva A, Richtand NW, Loftus J *et al*. Dopamine receptors in human adipocytes: expression and functions. *PLoS One* 2011; **6**: e25537.
6 Missale C, Nash SR, Robinson SW, Jaber M, Caron MG. Dopamine receptors: from structure to function. *Physiol Rev* 1998; **78**: 189–225.
7 Sidhu A, Niznik HB. Coupling of dopamine receptor subtypes to multiple and diverse G proteins. *Int J Dev Neurosci* 2000; **18**: 669–677.
8 Beaulieu JM, Gainetdinov RR. The physiology, signaling, and pharmacology of dopamine receptors. *Pharmacol Rev* 2011; **63**: 182–217.
9 Arcangeli S, Tozzi A, Tantucci M, Spaccatini C, de Iure A, Costa C *et al*. Ischemic-LTP in striatal spiny neurons of both direct and indirect pathway requires the activation of D1-like receptors and NO/soluble guanylate cyclase/cGMP transmission. *J Cereb Blood Flow Metab* 2013; **33**: 278–286.
10 Lin DT, Fretier P, Jiang C, Vincent SR. Nitric oxide signaling via cGMP-stimulated phosphodiesterase in striatal neurons. *Synapse* 2010; **64**: 460–466.
11 Natarajan A, Han G, Chen SY, Yu P, White R, Jose P. The d5 dopamine receptor mediates large-conductance, calcium- and voltage-activated potassium channel activation in human coronary artery smooth muscle cells. *J Pharmacol Exp Ther* 2010; **332**: 640–649.
12 Sharma RK, Duda T. Membrane guanylate cyclase, a multimodal transduction machine: history, present, and future directions. *Front Mol Neurosci* 2014; **7**: 56.
13 Evgenov OV, Pacher P, Schmidt PM, Haskó G, Schmidt HH, Stasch JP. NO-independent stimulators and activators of soluble guanylate cyclase: discovery and therapeutic potential. *Nat Rev Drug Discov* 2006; **5**: 755–768.
14 Azevedo MF, Faucz FR, Bimpaki E, Horvath A, Levy I, de Alexandre RB *et al*. Clinical and molecular genetics of the phosphodiesterases (PDEs). *Endocr Rev* 2014; **35**: 195–233.
15 Supuran CT, Mastrolorenzo A, Barbaro G, Scozzafava A. Phosphodiesterase 5 inhibitors--drug design and differentiation based on selectivity, pharmacokinetic and efficacy profiles. *Curr Pharm Des* 2006; **12**: 3459–3465.
16 Zhu B, Strada SJ. The novel functions of cGMP-specific phosphodiesterase 5 and its inhibitors in carcinoma cells and pulmonary/cardiovascular vessels. *Curr Top Med Chem* 2007; **7**: 437–454.
17 Zhang L, Zhang Z, Zhang RL, Cui Y, LaPointe MC, Silver B *et al*. Tadalafil, a long-acting type 5 phosphodiesterase isoenzyme inhibitor, improves neurological functional recovery in a rat model of embolic stroke. *Brain Res* 2006; **1118**: 192–198.
18 Flaim KE, Gessner GW, Crooke ST, Sarau HM, Weinstock J. Binding of a novel dopaminergic agonist radioligand [3H]-fenoldopam (SKF 82526) to D-1 receptors in rat striatum. *Life Sci* 1985; **36**: 1427–1436.
19 Murphy MB, Murray C, Shorten GD. Fenoldopam: a selective peripheral dopamine-receptor agonist for the treatment of severe hypertension. *N Engl J Med* 2001; **345**: 1548–1557.
20 Ng SS, Pang CC. In vivo venodilator action of fenoldopam, a dopamine D(1)-receptor agonist. *Br J Pharmacol* 2000; **129**: 853–858.
21 Weber RR, McCoy CE, Ziemniak JA, Frederickson ED, Goldberg LI, Murphy MB. Pharmacokinetic and pharmacodynamic properties of intravenous fenoldopam, a dopamine1-receptor agonist, in hypertensive patients. *Br J Clin Pharmacol* 1988; **25**: 17–21.
22 Bodei S, Arrighi N, Spano P, Sigala S. Should we be cautious on the use of commercially available antibodies to dopamine receptors? *Naunyn Schmiedebergs Arch Pharmacol* 2009; **379**: 413–415.
23 Michel MC, Wieland T, Tsujimoto G. How reliable are G-protein-coupled receptor antibodies? *Naunyn Schmiedebergs Arch Pharmacol* 2009; **379**: 385–388.
24 Granados-Principal S, Liu Y, Guevara ML, Blanco E, Choi DS, Qian W *et al*. Inhibition of iNOS as a novel effective targeted therapy against triple negative breast cancer. *Breast Cancer Res* 2015; **17**: 527.
25 Shen LH, Liao MH, Tseng YC. Recent advances in imaging of dopaminergic neurons for evaluation of neuropsychiatric disorders. *J Biomed Biotechnol* 20122012. 259349.
26 Almubarak M, Osman S, Marano G, Abraham J. Role of positron-emission tomography scan in the diagnosis and management of breast cancer. *Oncology (Williston Park)* 2009; **23**: 255–261.
27 Conole D, Scott LJ. Riociguat: first global approval. *Drugs* 2013; **73**: 1967–1975.
28 Carlo RD, Muccioli G, Bellussi G, Portaleoni P, Ghi P, Racca S. Steroid, prolactin, and dopamine receptors in normal and pathologic breast tissue. *Ann NY Acad Sci* 1986; **464**: 559–562.
29 Sachlos E, Risueño RM, Laronde S, Shapovalova Z, Lee JH, Russell J *et al*. Identification of drugs including a dopamine receptor antagonist that selectively target cancer stem cells. *Cell* 2012; **149**: 1284–1297.
30 Wang PS, Walker AM, Tsuang MT, Orav EJ, Glynn RJ, Levin R *et al*. Dopamine antagonists and the development of breast cancer. *Arch Gen Psychiatry* 2002; **59**: 1147–1154.
31 Zhao DL, Zou LB, Lin S, Shi JG, Zhu HB. Anti-apoptotic effect of esculin on dopamine-induced cytotoxicity in the human neuroblastoma SH-SY5Y cell line. *Neuropharmacology* 2007; **53**: 724–732.
32 Moreno-Smith M, Lu C, Shahzad MM, Pena GN, Allen JK, Stone RL *et al*. Dopamine blocks stress-mediated ovarian carcinoma growth. *Clin Cancer Res* 2011; **17**: 3649–3659.
33 Sarkar C, Chakroborty D, Chowdhury UR, Dasgupta PS, Basu S. Dopamine increases the efficacy of anticancer drugs in breast and colon cancer preclinical models. *Clin Cancer Res* 2008; **14**: 2502–2510.
34 Johnson DE, Ochieng J, Evans SL. The growth inhibitory properties of a dopamine agonist (SKF 38393) on MCF-7 cells. *Anticancer Drugs* 1995; **6**: 471–474.
35 Maggio R, Aloisi G, Silvano E, Rossi M, Millan MJ. Heterodimerization of dopamine receptors: new insights into functional and therapeutic significance. *Parkinsonism Relat Disord* 2009; **15**: S2–S7.
36 Goldstein DS, Swoboda KJ, Miles JM, Coppack SW, Aneman A, Holmes C *et al*. Sources and physiological significance of plasma dopamine sulfate. *J Clin Endocrinol Metab* 1999; **84**: 2523–2531.
37 Eisenhofer G, Coughtrie MW, Goldstein DS. Dopamine sulphate: an enigma resolved. *Clin Exp Pharmacol Physiol Suppl* 1999; **26**: S41–S53.
38 Ghosh D. Human sulfatases: a structural perspective to catalysis. *Cell Mol Life Sci* 2007; **64**: 2013–2022.
39 Dajani R, Cleasby A, Neu M, Wonacott AJ, Jhoti H, Hood AM *et al*. X-ray crystal structure of human dopamine sulfotransferase, SULT1A3. Molecular modeling and quantitative structure-activity relationship analysis demonstrate a

molecular basis for sulfotransferase substrate specificity. *J Biol Chem* 1999; **274**: 37862–37868.
40 Zaccolo M, Movsesian MA. cAMP and cGMP signaling cross-talk: role of phosphodiesterases and implications for cardiac pathophysiology. *Circ Res* 2007; **100**: 1569–1578.
41 Hoque KE, Indorkar RP, Sammut S, West AR. Impact of dopamine-glutamate interactions on striatal neuronal nitric oxide synthase activity. *Psychopharmacology (Berl)* 2010; **207**: 571–581.
42 Sammut S, Dec A, Mitchell D, Linardakis J, Ortiguela M, West AR. Phasic dopaminergic transmission increases NO efflux in the rat dorsal striatum via a neuronal NOS and a dopamine D(1/5) receptor-dependent mechanism. *Neuropsychopharmacology* 2006; **31**: 493–505.
43 Choi BM, Pae HO, Jang SI, Kim YM, Chung HT. Nitric oxide as a pro-apoptotic as well as anti-apoptotic modulator. *J Biochem Mol Biol* 2002; **35**: 116–126.
44 Proskuryakov SY, Gabai VL. Mechanisms of tumor cell necrosis. *Curr Pharm Des* 2010; **16**: 56–68.
45 Basu S, Sarkar C, Chakroborty D, Nagy J, Mitra RB, Dasgupta PS *et al*. Ablation of peripheral dopaminergic nerves stimulates malignant tumor growth by inducing vascular permeability factor/vascular endothelial growth factor-mediated angiogenesis. *Cancer Res* 2004; **64**: 5551–5555.
46 Basu S, Nagy JA, Pal S, Vasile E, Eckelhoefer IA, Bliss VS *et al*. The neurotransmitter dopamine inhibits angiogenesis induced by vascular permeability factor/vascular endothelial growth factor. *Nat Med* 2001; **7**: 569–574.
47 Chakroborty D, Sarkar C, Basu B, Dasgupta PS, Basu S. Catecholamines regulate tumor angiogenesis. *Cancer Res* 2009; **69**: 3727–3730.
48 Sarkar C, Chakroborty D, Mitra RB, Banerjee S, Dasgupta PS, Basu S. Dopamine in vivo inhibits VEGF-induced phosphorylation of VEGFR-2, MAPK, and focal adhesion kinase in endothelial cells. *Am J Physiol Heart Circ Physiol* 2004; **287**: H1554–H1560.

Supplementary Information accompanies this paper on the Oncogene website (http://www.nature.com/onc)